

ASFM Discharge Measurements at CNR's Montélimar and Beauchastel Hydropower Plants

D. Billenness¹, P. Roumieu², J. Buermans¹, D. Lemon¹

¹ASL Environmental Sciences Inc., 1 – 6703 Rajpur Pl., Victoria, BC, Canada

²Compagnie Nationale du Rhône, Lyon, France

E-mail (corresponding author): dbillenness@aslenv.com

Abstract

Compagnie Nationale du Rhône (CNR) conducted Acoustic Scintillation Flow Meter (ASFM) measurements in each of the three intake bays at Unit 6 and Unit 2 at the Montélimar hydroelectric plant in 2021 and 2022. Detailed 30-path measurements in each intake bay were used to select the optimal positions of the ASFM paths for subsequent 3-bay 10-path ASFM measurements.

In 2023, CNR extended their investigation to Unit 5 at the Beauchastel plant, employing two combined 10-path ASFM instruments to conduct extensive 3-bay, 20-path measurements.

This paper presents the ASFM measurement device and associated methodology in detail. The process of selecting 10 paths from the initial 30 paths is described. Finally, a comparative analysis of flow measurements obtained from both the 30-path and 10-path configurations at Montélimar, as well as the 20-path measurements at Beauchastel, is provided.

1. Introduction

CNR is a major component of France's electrical power system, with 4000 MW of 100% renewable capacity. Seventy-five percent of that capacity is hydroelectric generation and CNR has undertaken a major optimization project to maximize its production. As part of that project, CNR has been making performance measurements on many of its units to assess whether there is potential to improve performance by adjusting operating parameters, or if they should be replaced with new turbines. Many of the CNR plants are low-head, with either Kaplan or bulb turbines, and therefore have limited options for flow measurements required to measure unit performance. CNR has been using the acoustic scintillation method in the unit intakes to make those measurements, because of its relatively short time to complete a discharge measurement and its portability between intakes of similar design.

Most methods for making flow measurements in an intake sample the velocity field at a number of fixed elevations over the height of the intake, which is the case for acoustic scintillation. The number and location of those measurement elevations needed to measure the discharge to the desired accuracy depends on the complexity of the velocity field at the measurement plane. The number of measurement paths may be minimized by selecting their elevations so that measuring the velocity at those locations will produce an accurate discharge when numerically integrated. Here, initial 30-elevation measurements were made to define the intake velocity profile in detail. A subset of 10 of those elevations was then selected for the subsequent data collection program.

2. Acoustic Scintillation Method

2.1 Principle of Operation

The ASFM uses a technique called acoustic scintillation drift (Clifford & Farmer, 1983; Farmer & Clifford, 1986; ASL, 2001) to measure the flow velocity perpendicular to a number of acoustic paths established across the intake to the turbine. Short pulses (16µsec) of high-frequency sound (307 kHz) are sent from transmitting arrays on one side to receiving arrays on the other, at a rate of approximately 250 pings /second. Fluctuations in the amplitude of those acoustic pulses result from turbulence in the water carried along by the current. The ASFM measures those fluctuations (known as scintillations) and from them computes the lateral average (i.e. along the acoustic path) of the velocity perpendicular to each path.

In its simplest form, two transmitters are placed on one side of the measurement section, two receivers at the other. The signal amplitude at the receivers varies randomly as the turbulence along the propagation paths changes with time and the flow. If the two paths are sufficiently close (Δx), the turbulence remains embedded in the flow, and the pattern of these amplitude variations at the downstream receiver will be nearly identical to that at the upstream receiver, except for a time

delay, Δt , which corresponds to the peak in the time-lagged cross-correlation function calculated for the two signals. The mean velocity perpendicular to the acoustic paths is then $\Delta x/\Delta t$. Using three transmitters and three receivers (in a triangular array) at each measurement level allows both the magnitude and inclination of the velocity to be measured. The ASFM computes the discharge through each bay of the intake by integrating the horizontal component of the velocity over the cross-sectional area of the intake. The discharges through each bay are then summed to compute the total discharge.

3. Diagnostic Measurements at Montélimar

3.1 30-path Installation

In February 2021, unit performance measurements were begun at Unit 6 (G6) of the Châteauneuf du Rhône-Montélimar-Henri Poincaré (Montélimar) power plant on the Rhône River, a Kaplan unit with a 3-bay intake. To define the velocity profile, an initial set of measurements using 30 levels was made in each of the three bays. Vertical section views of the intake at Montélimar are shown in Figures 1 and 2. The ASFM sensors were installed in the stoplog slot, as indicated in Figures 3 and 4. At the stoplog slot, each bay is 5.4m wide and 12.3m high.

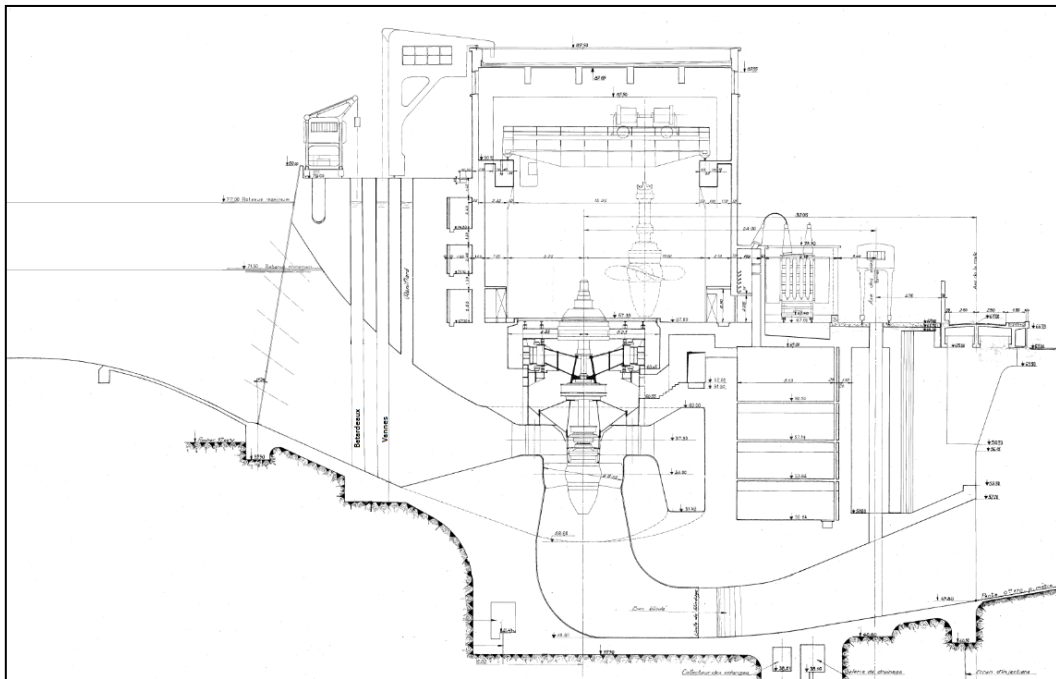


Figure 1: Vertical cross-section of Montélimar intake.

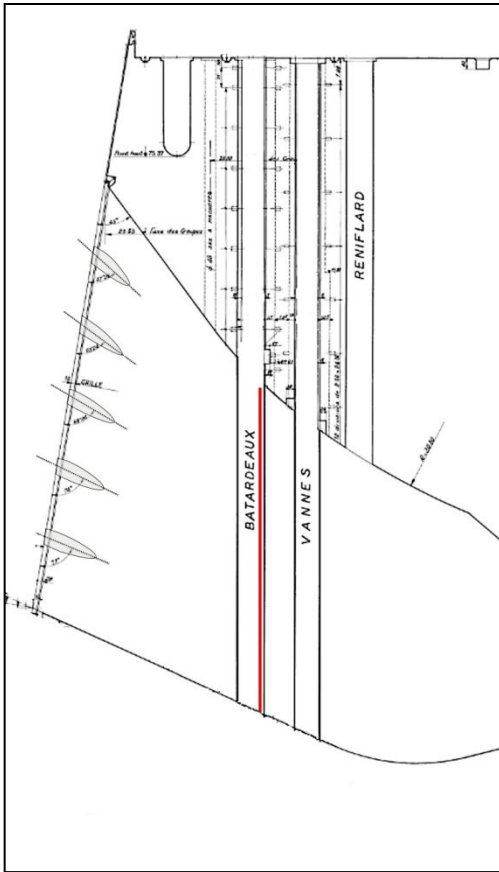


Figure 2: Location (in Red) of the ASFM sensor plane in G6 intake

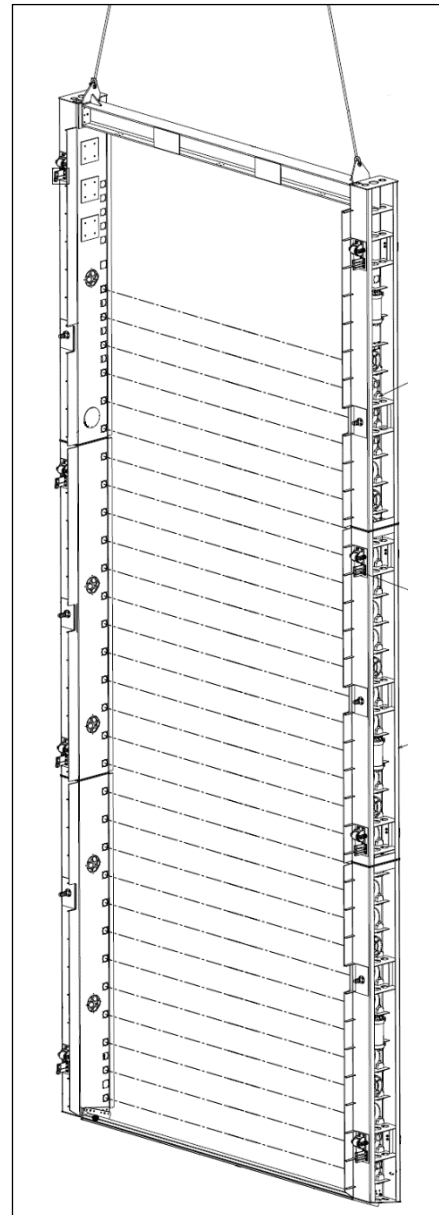


Figure 3: Schematic of the flow measurement frame

Diagnostic measurements were needed to resolve the water velocity variations at the instrument measurement plane. The trashrack support structure includes 5 large horizontal supports shown in Figure 2. Since CNR's equipment included only 30 ASFM transducer pairs, 10 transducer positions needed to be selected for each of the 3 frames – one set for each intake bay. A schematic of the frame is shown in Figure 3, and the path layout of the ASFM arrays on the frame and definition of associated parameters are shown in Figure 4. The rows of holes for the ASFM transducers were placed close to the downstream edge of the slot; the centerline of the arrays was 17 cm upstream of the concrete edge. The transducers were placed with their faces flush with the sides of the frame so that the full width of the intake was sampled and that they were protected from any debris carried along with the flow.

Forty pairs of holes for the arrays were provided on the frame to deal with the different height at the 4 plants for which the frames were designed. The 6 pairs of holes near the bottom and the 12 pairs near the top of the frame were spaced 20cm apart to help resolve large variations that typically occur there. In the center portion of the frame, pairs of holes were spaced approximately 40cm apart. 30 pairs were selected for the diagnostic measurements.

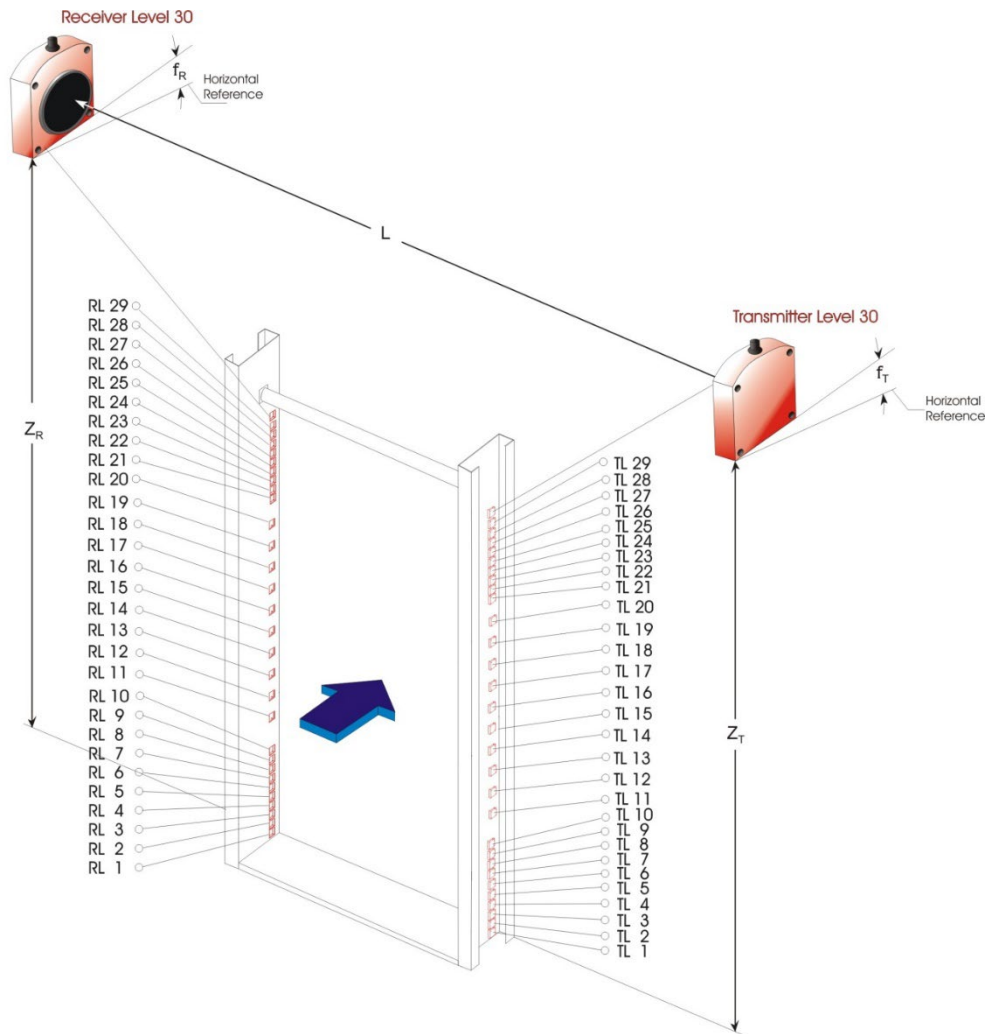


Figure 4: Schematic diagram of the components of the 30-path ASFM system.

There were 4 repeats made at a nominal $Q=200 \text{ m}^3/\text{s}$ in each bay at all 30 levels. The average discharge was computed from the average of the velocities at each level from each of the individual runs. Boundary conditions on the velocity profile at the floor and roof for the discharge calculation were set as follows:

Floor: $V(z) = V(T) * (z/T)^{1/X}$, where z is the elevation above the floor and T is the boundary layer thickness.

Roof: $V(z) = V(Z_r - T) * [(Z_r - z)/T]^{1/X}$, where Z_r is the elevation of the roof. Values used for these parameters are listed in Table 1.

Table 1: Boundary conditions used for the 30-path measurements

Bay	Roof (Entered Thickness)		Floor		Zroof (m)	Zfloor (m)
	X	T (m)	T (m)	X		
1	7	0.4	0.3	7	12.272	0
2	7	0.4	0.3	12	12.278	0
3	7	0.4	0.3	12	12.264	0

The computed discharges for each bay, the total discharge and the calculated relative uncertainty are listed in Table 2; the corresponding vector and horizontal velocity profiles for each bay are shown in Figures 5 – 7.

The relative uncertainty in the discharge is computed from the random uncertainty in the horizontal velocity. Each velocity estimate is computed from a set of 8.2-second samples (2048 points), which are then averaged. Here, each set comprised

4 samples, for a 32-second measurement. The standard deviation of the average horizontal velocity, V_h , computed from each of the 8.2-second blocks is given by σ . Averaging N blocks reduces the random error relative to the individual sample errors by $1/\sqrt{N}$. The relative uncertainty in the horizontal velocity computed from each of the four repeat runs as is then:

$$\Delta v = \frac{\sigma}{V_h \cdot \sqrt{N}}$$

The random error is further reduced by averaging the repeat runs together. The average relative uncertainty at each level is calculated from the 4-repeat runs as:

$$\overline{\Delta v} = \frac{\sqrt{(\Delta v_1 \cdot V_{h1})^2 + (\Delta v_2 \cdot V_{h2})^2 + (\Delta v_3 \cdot V_{h3})^2 + (\Delta v_4 \cdot V_{h4})^2}}{\overline{V_h}}$$

where $\Delta v_1, \Delta v_2, \Delta v_3$ and Δv_4 are the individual relative uncertainties from the repeat runs, V_{h1}, V_{h2}, V_{h3} and V_{h4} are the horizontal velocities of the repeat runs, and $\overline{V_h}$ is the average horizontal velocity computed from the repeat runs. The average horizontal velocities are then integrated numerically over the height of the intake (using an adaptive Romberg integration: Press et al, 1986) to give the discharge, Q . The relative random error in Q is then

$$\frac{\Delta Q}{Q} = \frac{\sqrt{\sum_1^N w_i^2 \cdot \sigma_i^2}}{\sum_1^N w_i \cdot V_{hi}}$$

where $\sigma_i = \overline{\Delta v_i} \cdot \overline{v_i}$ is the standard deviation of the i^{th} average horizontal velocity, V_{hi} , and the weighting factor w_i represents the fraction of the total area of the intake that path i measures. The relative uncertainty in all three bays was under 0.5%. These results were then used for the selection of the 10 paths.

Table 2: Results of 4-repeat runs using 30-path ASFM measurements at $Q=200m^3/s$

	Bay 1	Bay 2	Bay 3	Qtotal
Q (m³/s)	71.50	65.90	62.48	199.88
Rel. Uncertainty (%)	0.64	0.44	0.49	0.31

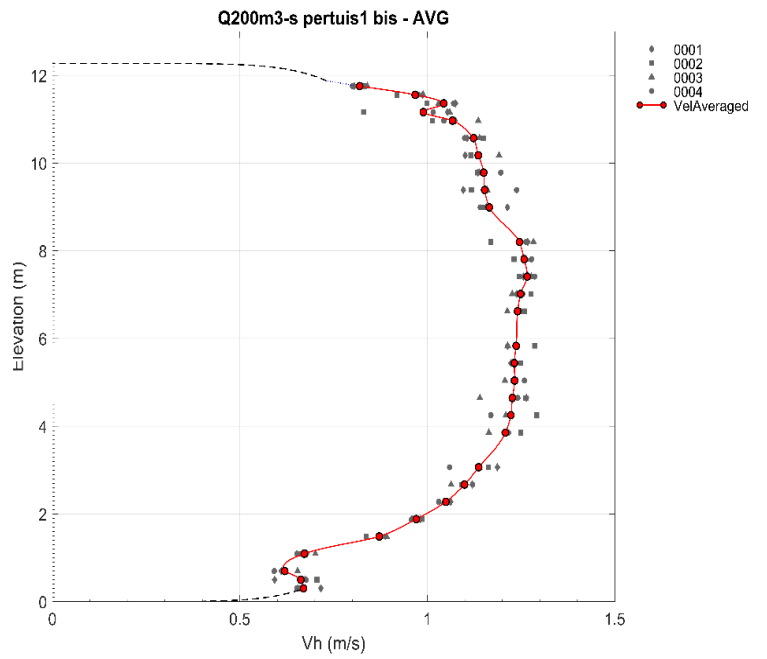
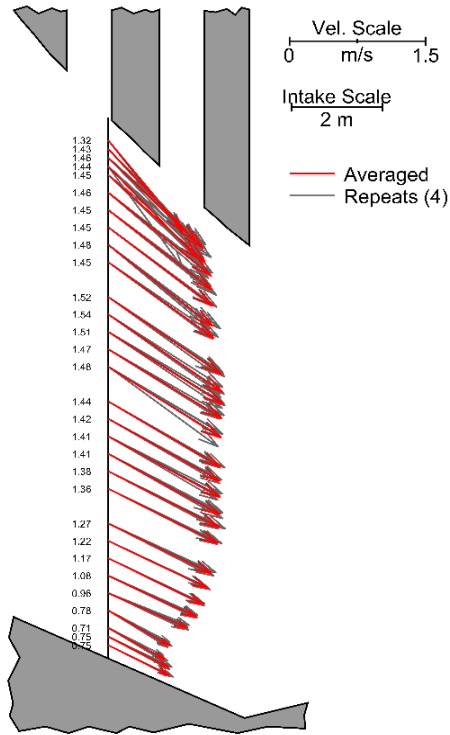


Figure 5: Velocity profiles for Bay 1 at $Q = 200 \text{ m}^3/\text{s}$

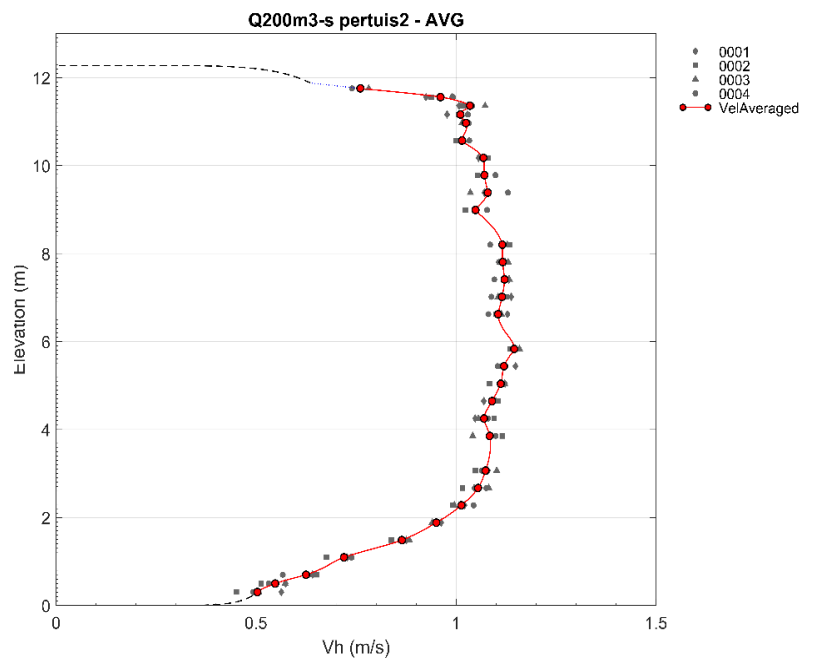
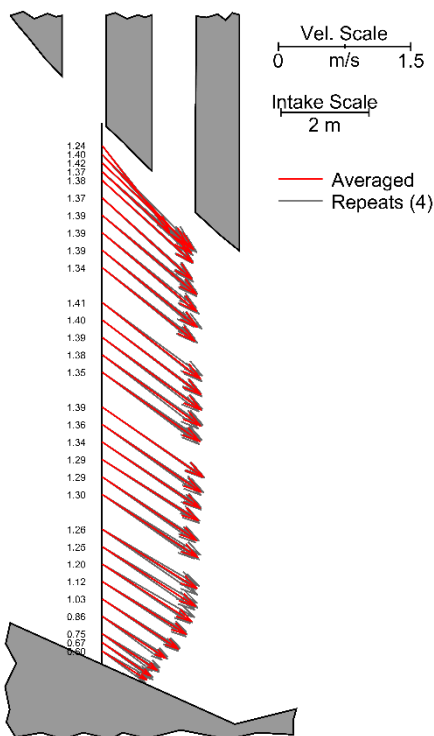


Figure 6: Velocity profiles for Bay 2 at $Q = 200 \text{ m}^3/\text{s}$

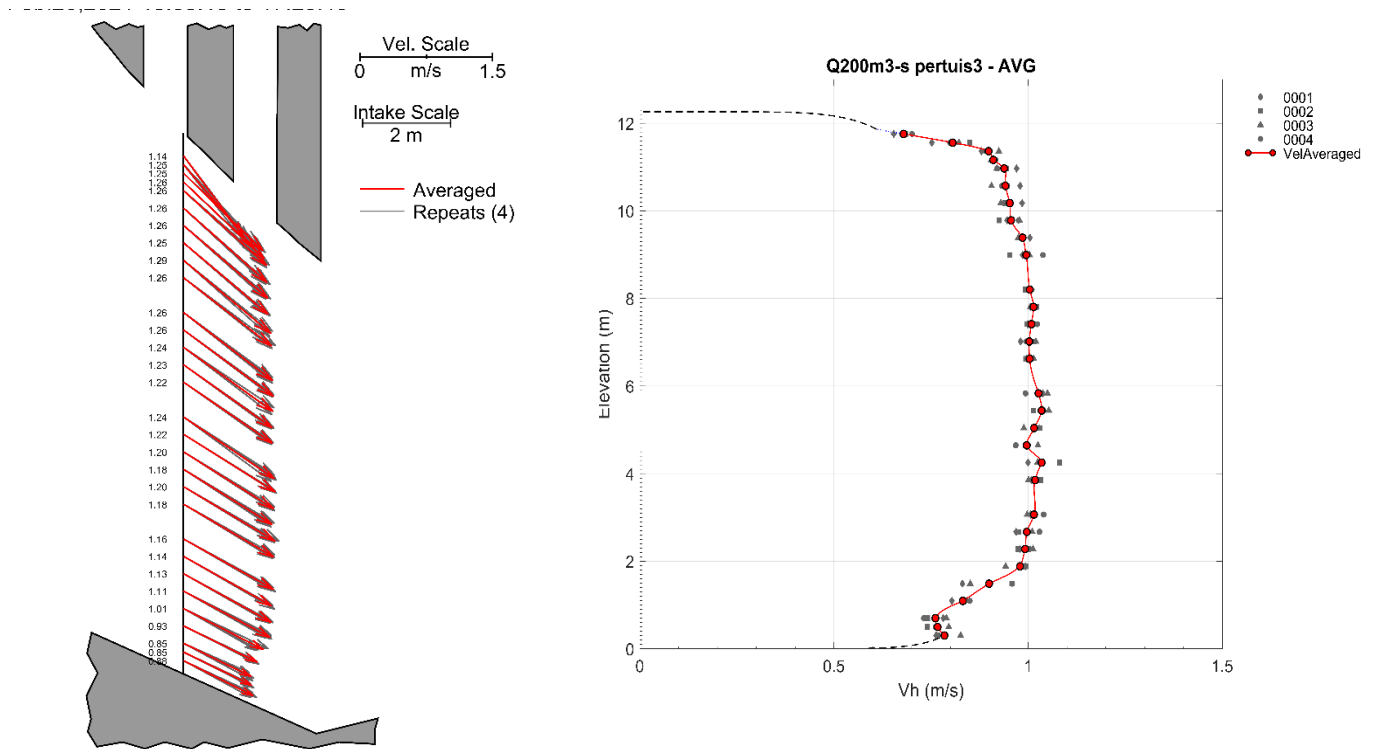


Figure 7: Velocity profiles for Bay 3 at $Q = 200 \text{ m}^3/\text{s}$

3.2 Selection of the 10-path elevations.

The profile of the horizontal component of velocity measured in each bay was reviewed, and three 10-path options were selected from them. The discharges computed using each option (using modified boundary conditions) were compared with the value calculated using all 30 paths. Option 1 used one set of elevations in Bays 1 & 2, and a slightly different set for Bay 3. The second and third options used the same elevations for all three bays. The positions of the 10-path subsets are shown in Figures 8, 9 and 10; the boundary conditions for each 10-path option are shown in Tables 3, 4 and 5. Table 6 summarizes the individual bay and total discharges from each 10-path option along with the reference discharges from the 30-path measurements.

Table 3: Option 1- Boundary conditions

Bay	Roof (Entered Thickness)		Floor		Zroof (m)	Zfloor (m)
	X	T (m)	T (m)	X		
1	6	0.52	0.7	6	12.272	0
2	6	0.52	0.7	6	12.278	0
3	6	0.52	0.7	6	12.264	0

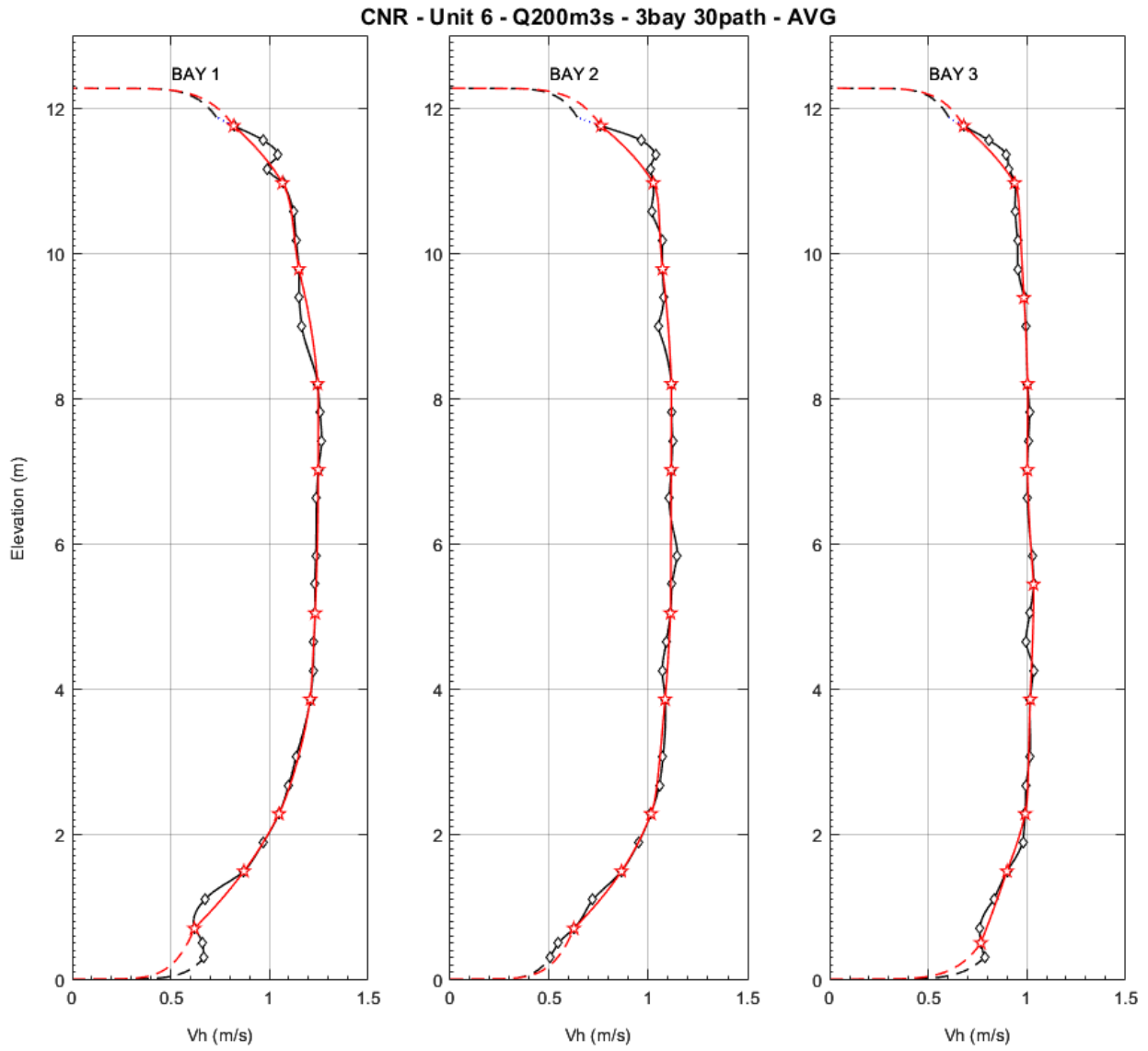


Figure 8: Option 1 - 30 path measurements (black) and 10 path selection (red)

Table 4: Option 2 boundary conditions

Bay	Roof (Entered Thickness)		Floor		Zroof (m)	Zfloor (m)
	X	T (m)	T (m)	X		
1	6	0.52	0.7	12	12.272	0
2	6	0.52	0.7	12	12.278	0
3	6	0.52	0.7	12	12.264	0

CNR - Unit 6 - Q200m3s - 3bay 30path - AVG

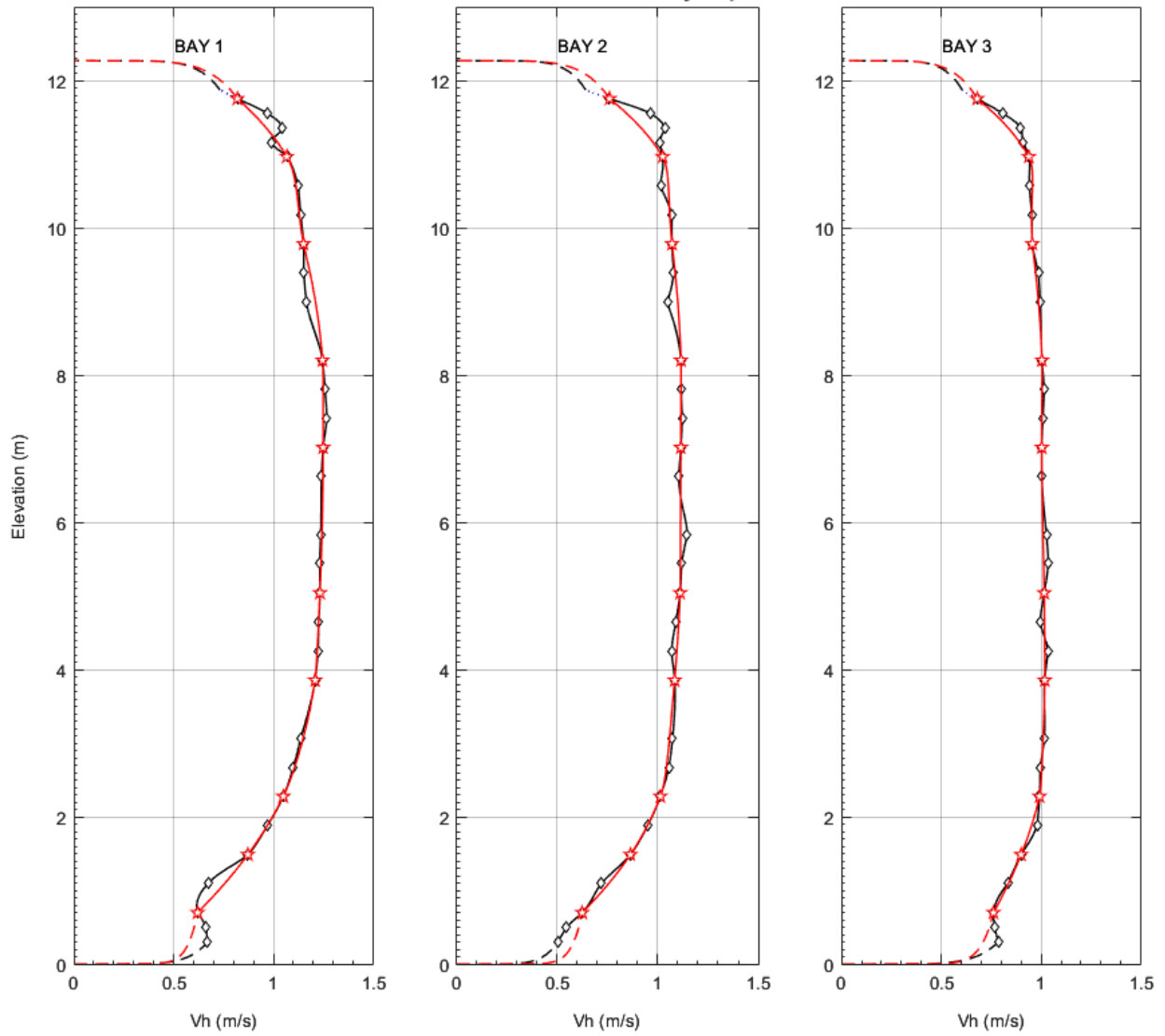


Figure 9: Option 2 - 30 path measurements (black) and 10 path selection (red)

Table 5: Option 3 boundary conditions.

Bay	Roof (Entered Thickness)		Floor		Zroof (m)	Zfloor (m)
	X	T (m)	T (m)	X		
1	6	0.52	0.7	6	12.272	0
2	6	0.52	0.7	6	12.278	0
3	6	0.52	0.7	6	12.264	0

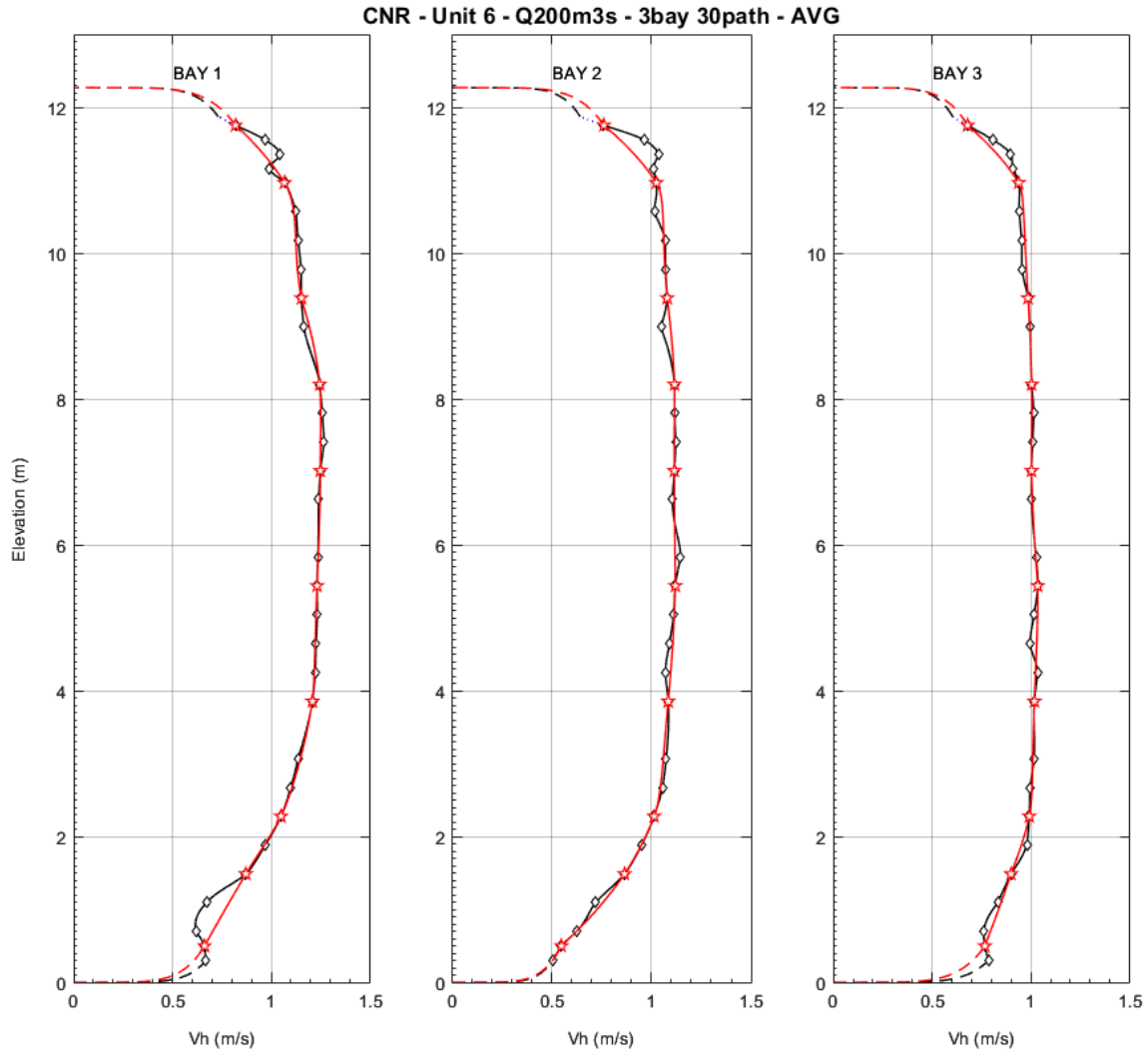


Figure 10: Option 3 - 30 path measurements (black) and 10 path selection (red)

Table 6: Discharge Q , relative uncertainty δ , and relative differences in total discharge from the 30-path reference for each 10-path option.

	30 path		Option 1		Option 2		Option 3		% Difference 10path : 30path		
	Q (m^3/s)	δ (%)	Option 1	Option 2	Option 3						
Bay 1	71.50	0.64	71.53	0.96	71.68	0.96	71.70	0.96	0.04	0.25	0.28
Bay 2	65.90	0.44	66.05	0.76	66.20	0.76	65.94	0.76	0.23	0.46	0.06
Bay 3	62.48	0.49	62.42	0.78	62.07	0.78	62.42	0.78	-0.10	-0.66	-0.10
Total	199.88	0.31	199.99	0.49	199.96	0.49	200.06	0.55	0.06	0.04	0.09

In each case, the total discharge computed using 10 paths differed from the 30-path result by less than 0.1%. The relative uncertainty in each 10-path result was approximately 60% larger than was the case for the 30-path measurements. The first option was chosen for the locations of the subsequent 3-bay 10-path measurement program as having the least overall differences for the individual bay discharges; however, the third option was also a good choice.

4. 20-path measurements at Beauchastel

4.1 Measurement Plan

In July 2023, CNR began flow measurements at Unit G5 in the Beauchastel power plant on the Rhône River. Beauchastel is a low-head, short intake plant equipped with Kaplan turbines, so acoustic scintillation in the intake was selected as the measurement method. At the measurement plane, the intake is 13.3 metres high and 5.4 metres wide. Because of the size of the intake, achieving the required discharge accuracy with the standard 10 path ASFM system would normally require preliminary 30-path diagnostic measurements, as was done at Montélimar, to determine the optimal path placement. The diagnostic measurements are labour-intensive and time-consuming, as they must be done separately for each intake bay. In this case, CNR elected instead to use two ASFM instruments to deploy 20 paths in each bay to eliminate the preliminary diagnostic tests.

4.2 Beauchastel Installation

The ASFM typically is divided into 3 groups for operation in multi-bay intakes; each group consists of 10 levels (transducers in pairs of Tx and Rx), two switching canisters, and cabling. A schematic of the two ASFM's that were installed at G5 is shown in Figure 11.

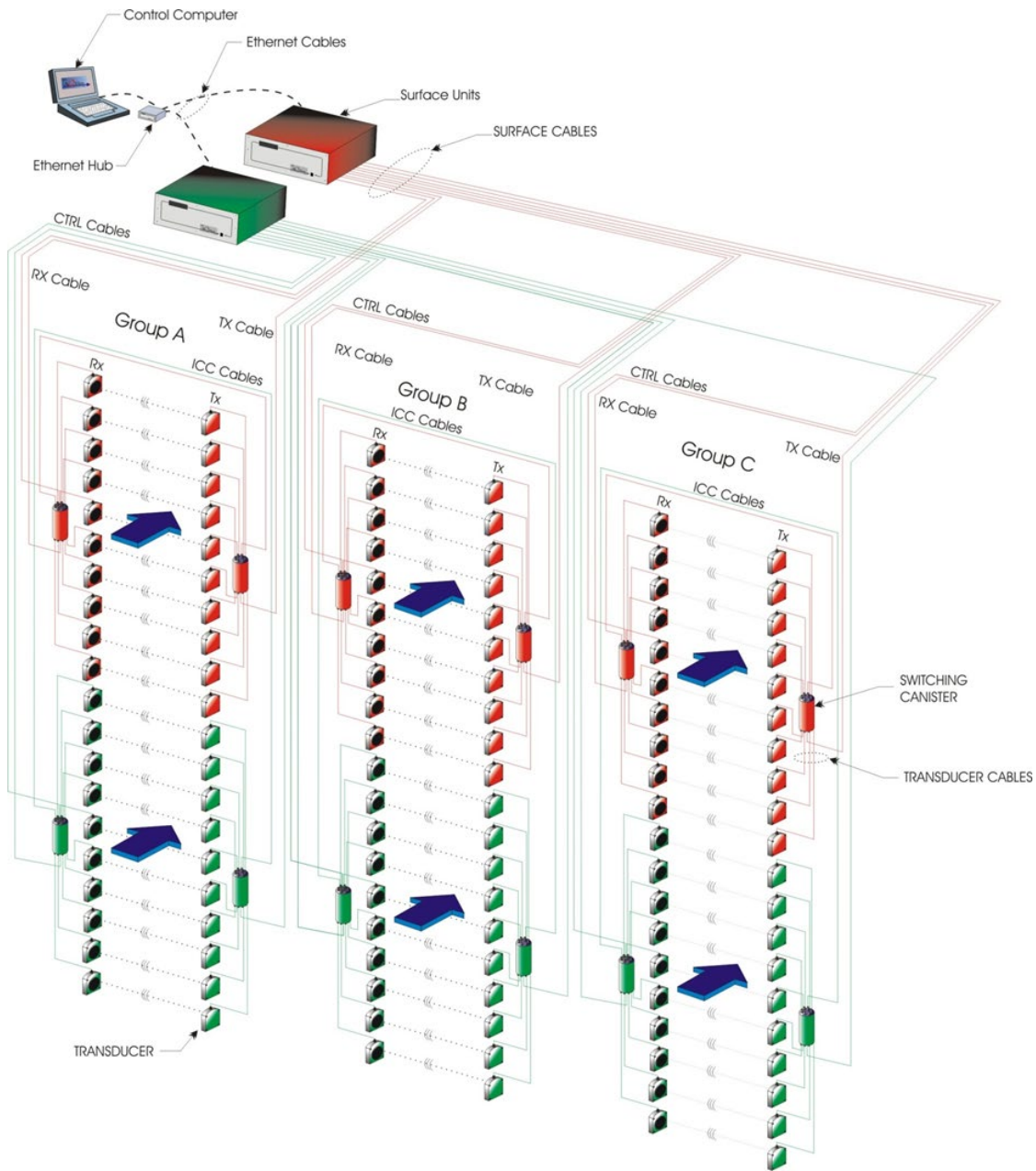


Figure 11: 3-bay, 20 path ASFM with 2 surface units

The two surface units were connected to an Ethernet switch and, using ASFM Link, it allowed the simultaneous collection of two levels and three groups (two levels in each bay e.g. Level 1 green and Level 1 red in Bays A, B and C). When using two surface units, the data collection time for a complete measurement is the same as for a 3-bay, 10-path system.

4.3 Data Collection

Preliminary measurements were carried out in July to test the performance of the 20-path/bay system. The velocity vector plots are shown in Figure 12. Overall, the data quality from the 20-path data in each bay was very good apart from Levels 1-3 in Bay B and Level 1 in Bay C where standard deviation of the horizontal velocity was over 10%. This was likely due to a blockage (sediment) at the bottom of the trash racks in these two bays. Despite the poor data quality at these bottom levels, the standard deviation of the repeat runs divided by the average discharge was 0.3% for Runs 1-13 (using the standard 4 repeats: Run 1-4 0.30%, Run 5-8 0.32%, and Run 9-13 0.32%). This was taken to indicate that 30-path diagnostic measurements are not necessary when using a 20-path, 3-bay system.

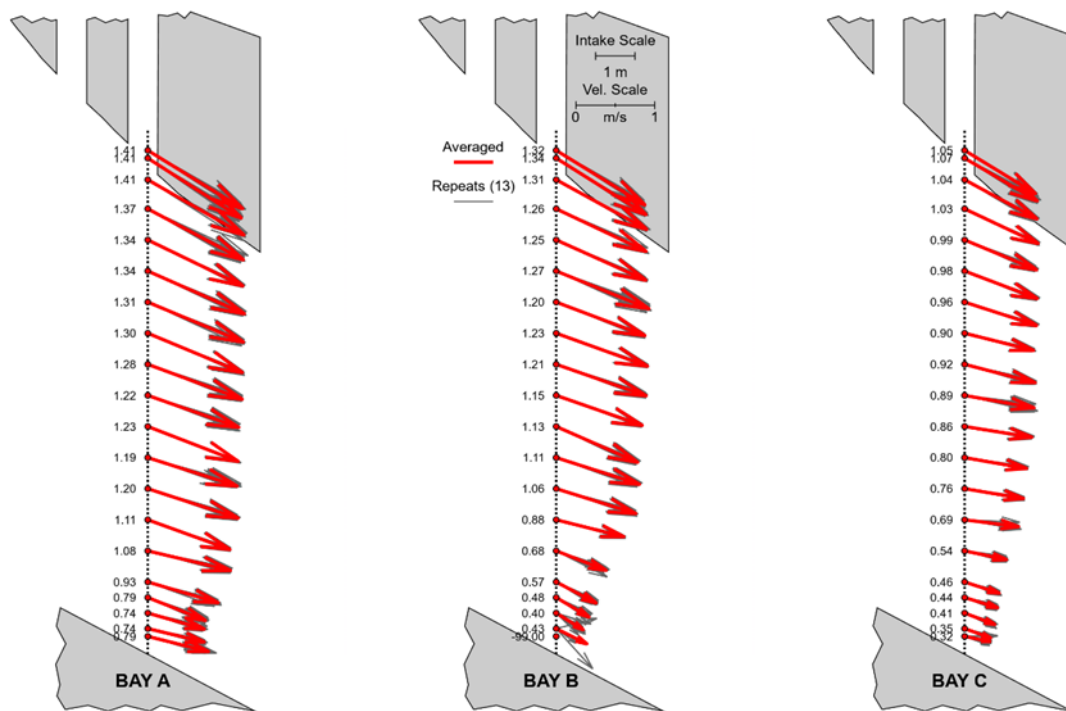


Figure 12: Velocity vector plots from 13 repeats runs at $Q = 200 \text{ m}^3/\text{s}$. The red vectors in the vector plots represent the averaged velocity with the value shown in text in m/s. The grey vectors are each of the velocities measured during the repeat runs.

A full set of measurements with 20 paths per bay were collected in January 2024, using a sampling time of 50 seconds per level with 4 repeat runs for most settings. The results are shown in Table 7. Figures 13 and 14 show sample vector and horizontal velocity plots for the nominal $300 \text{ m}^3/\text{s}$ run. Some evidence of blockage is still apparent at the bottom of the central bay, however it does not seem to have affected the quality of the flow data, as the standard deviation of the total discharge over the repeat runs was $\leq 0.52\%$ in all cases.

Table 7: Discharges by Bay and total discharge and standard deviation, January 2024.

Nominal Q (m ³ /s)	# repeat runs	Bay A	Bay B	Bay C	Total	
		Q (m ³ /s)	σ (%)			
100	2	41.69	38.34	29.08	109.11	0.52
120	2	49.51	45.63	34.04	129.18	0.38
140	3	56.54	50.45	39.14	146.13	0.39
160	5	63.10	56.42	43.55	163.07	0.25
180	4	70.26	62.87	49.39	182.52	0.32
200	4	78.91	70.57	55.52	205.00	0.28
220	4	85.70	76.53	60.43	222.66	0.27
240	4	95.99	83.50	67.48	246.97	0.29
260	4	104.39	91.50	73.03	268.91	0.51
280	4	112.76	99.17	79.33	291.26	0.22
300	4	120.72	104.88	83.88	309.47	0.19
320	4	131.49	112.43	92.99	336.91	0.38
340	4	137.22	121.45	94.94	353.61	0.24

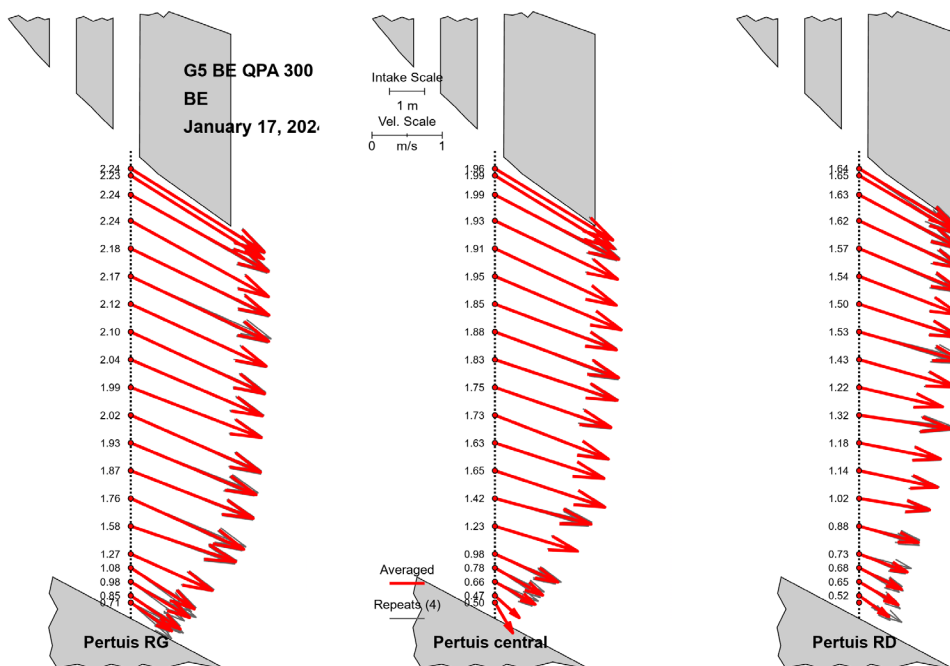


Figure 13: Velocity vector plot, nominal $Q = 300 \text{ m}^3/\text{s}$.

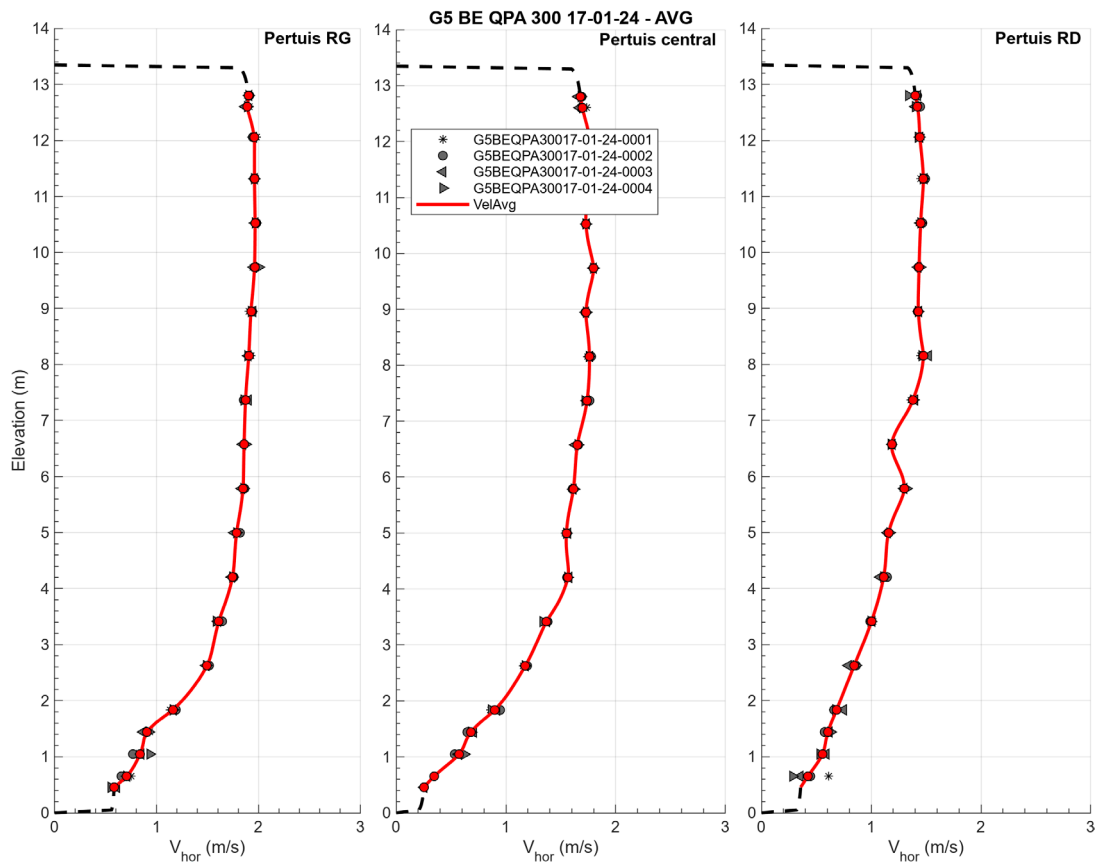


Figure 14: Horizontal velocity plot, nominal $Q = 300 \text{ m}^3/\text{s}$.

5. Conclusions

Two methods for adequately sampling the velocity field in large intakes over 10 metres in height using the acoustic scintillation method were evaluated at two Kaplan plants on the Rhône River. At the Montélimar plant, 30 acoustic paths were used to intensively sample the velocity profile in each of the 3 intake bays to select subsets of 10 for the ensuing program. This approach minimized the instrumentation required (only one standard 30-path ASFM unit) but at the cost of additional labour and time needed to move the system from bay to bay and then to select the path subsets. Using two instrument systems to install 20 paths in each bay, as was done at Beauchastel, produced data of equal quality with less time and labour, which would continue to be realized in future work. CNR has decided to proceed with the double instrument approach in future.

References

- ASL Environmental Sciences Inc., 2001. Acoustic Scintillation Flow Meter: Operating Manual for Advantage Model. ASL Environmental Sciences Inc., Sidney, BC, Canada.
- Clifford, S. F. and D. M. Farmer, 1983. Ocean flow measurements using acoustic scintillation. *J. Acoust. Soc. Am.* **74** (6), 1826 – 1832.
- Farmer, D. M. and S. F. Clifford, 1986. Space-time acoustic scintillation analysis: a new technique for probing ocean flows. *IEEE J. Ocean Eng.* OE-11 (1), 42-50.
- Press, W. H., B. P. Flannery, S. A. Teukolsky and W. T. Vetterling. 1986. *Numerical Recipes: The Art of Scientific Computing*, Cambridge University Press, Cambridge.